LETTER • OPEN ACCESS

Lack of vegetation exacerbates exposure to dangerous heat in dense settlements in a tropical African city

View the article online for updates and enhancements.

ENVIRONMENTAL RESEARCH
LETTERS

LETTER

Lack of vegetation exacerbates exposure to dangerous heat in dense settlements in a tropical African city

J Van de Walle[1,*] , O Brousse[1,2] , L Arnalsteen[1], C Brimicombe[3] , D Byarugaba[4], M Demuzere[5] ,
E Jjemba[6], S Lwasa[4] , H Misiani[7] , G Nsangi[8] , F Soetewey[1], H Sseviiri[4], W Thiery[9] , R Vanhaeren[1],
B F Zaitchik[10] and N P M van Lipzig[1]

1 KU Leuven, Leuven, Belgium
2 University College London, London, United Kingdom
3 University of Reading, Reading, United Kingdom
4 Makerere University, Kampala, Uganda
5 Ruhr-University Bochum, Bochum, Germany
6 Red Cross Red Crescent Climate Centre, The Hague, Netherlands
7 IGAD Climate Prediction and Applications Centre (ICPAC), Nairobi, Kenya
8 University of Oklahoma, Norman, OK, United States of America
9 Vrije Universiteit Brussel, Brussels, Belgium
10 Johns Hopkins University, Baltimore, MD, United States of America
* Author to whom any correspondence should be addressed.

E-mail: jonas.vandewalle@kuleuven.be

Abstract
Both climate change and rapid urbanization accelerate exposure to heat in the city of Kampala, Uganda. From a network of low-cost temperature and humidity sensors, operational in 2018–2019, we derive the daily mean, minimum and maximum Humidex in order to quantify and explain intra-urban heat stress variation. This temperature-humidity index is shown to be heterogeneously distributed over the city, with a daily mean intra-urban Humidex Index deviation of 1.2 °C on average. The largest difference between the coolest and the warmest station occurs between 16:00 and 17:00 local time. Averaged over the whole observation period, this daily maximum difference is 6.4 °C between the warmest and coolest stations, and reaches 14.5 °C on the most extreme day. This heat stress heterogeneity also translates to the occurrence of extreme heat, shown in other parts of the world to put local populations at risk of great discomfort or health danger. One station in a dense settlement reports a daily maximum Humidex Index of >40 °C in 68% of the observation days, a level which was never reached at the nearby campus of the Makerere University, and only a few times at the city outskirts. Large intra-urban heat stress differences are explained by satellite earth observation products. Normalized Difference Vegetation Index has the highest (75%) power to predict the intra-urban variations in daily mean heat stress, but strong collinearity is found with other variables like impervious surface fraction and population density. Our results have implications for urban planning on the one hand, highlighting the importance of urban greening, and risk management on the other hand, recommending the use of a temperature-humidity index and accounting for large intra-urban heat stress variations and heat-prone districts in urban heat action plans for tropical humid cities.

1. Introduction

Heat is a killer hazard with a global reach. Its exposure has been associated with both increased mortality and morbidity worldwide (Medina-Ramón and Schwartz 2007, Oudin Åström *et al* 2011, Fischer *et al* 2012, Mora *et al* 2017), raising serious concerns for human health in a projected warmer future climate (Kovats and Hajat 2008, Huang *et al* 2011, Guo *et al* 2014, Mora *et al* 2017). Former research on health

impact of extreme heat concentrates on mid-latitude, high-income countries of low to medium population density (Campbell *et al* 2018, Green *et al* 2019, Otto *et al* 2020), thereby chronically underreporting regions that are projected to actually experience the most extreme heat in the future (Im *et al* 2017, Mora *et al* 2017, Nagendra *et al* 2018, Harrington and Otto 2020, Saeed *et al* 2021). For example, Africa is particularly vulnerable to heat stress (IPCC 2014, Singh *et al* 2019). A rapid increase in the intensities and frequencies of heatwaves during the past decades has been demonstrated (Ceccherini *et al* 2017, Amou *et al* 2021), while simulations project this trend to continue uninterrupted into the future (Harrington *et al* 2016, Russo *et al* 2016, Dosio *et al* 2018). For instance, under a higher emission scenario (SSP5-8.5), Africa's exposure to extreme heat is projected to be 7–269 times larger than it has been historically (Liu *et al* 2017, Asefi-Najafabady *et al* 2018).

Extreme heat is further amplified in cities, which are shown to be warmer than their natural surroundings, because of reduced vegetated areas, increased release of anthropogenic heat, changes in surface albedo and trapped radiation within street canyons (Oke 1982). This urban heat island effect has also been demonstrated for Sub-Saharan African cities (Nakamura 1966, Jonsson *et al* 2004, Roth 2007, Brousse *et al* 2020), experiencing rapid population growth (McGranahan and Satterthwaite 2014, United Nations 2019) and extensive urbanization (Liu *et al* 2017, United Nations 2018, Marcotullio *et al* 2021). As an example, Kampala, the capital city of Uganda, is experiencing an uncontrolled urbanization, having the fourth highest growth rate ($>4\%\,\mathrm{yr}^{-1}$) of all African cities (Richmond *et al* 2018, Kampala Capital City Authority and Uganda Bureau of Statistics 2019). Like many fast-growing cities, Kampala is expanding horizontally (Brousse *et al* 2019, Li *et al* 2021), demonstrating spatial patterns of urban sprawl (Vermeiren *et al* 2016, Hemerijckx *et al* 2020) and the formation of informal settlements or slums (Van Leeuwen *et al* 2017, Lwasa *et al* 2018, Richmond *et al* 2018).

Within the city of Kampala, both morphological and socio-economical characteristics largely differ, distinguishing wealthy districts characterized by asphalted roads, modern houses and large gardens, from informal settlements composed of densely built shacks made of corrugated metal sheets that are only accessible via small alleys (Vermeiren *et al* 2012, Hemerijckx *et al* 2020). Recently, Brousse *et al* (2019) classified these intra-urban variations into Local Climate Zones (LCZ, Stewart and Oke 2012). This classification includes 7 vegetated and 10 built classes, each class exemplifying uniform surface cover, structure, material and human activity that span hundreds of meters to several kilometers in horizontal scale (Stewart 2011). Importantly, LCZs are designed to reflect the thermal environments as a consequence of their

intra-urban variations. LCZ are thus expected to also reflect heat stress variations in the city (Kabano *et al* 2021, Van de Walle *et al* 2021), similar to the findings in Nairobi (Kenya), concluding that informal settlements are particularly prone to heat stress (Scott *et al* 2017).

However, observational studies investigating this heterogeneity have been depreciated, because of the characteristic meteorological data scarcity in the region (Roth 2007). Six weather stations were set up in Kampala only recently, thanks to the Trans-African Hydro-Meteorological Observatory (TAHMO, van de Giesen *et al* 2014) project, collecting meteorological data from the synoptic station at Makerere university and five instrument shelters placed in open school gardens, in accordance with the official World Meteorological Organization standards (WMO 1986). Despite this great observational effort, no stations are placed in more densely built environments where most of Kampala's population lives.

To better represent the variations of heat stress throughout the city of Kampala, including densely populated areas, this study put in place an observational network of 45 low-cost iButton sensors. These sensors recorded near-surface air temperature and relative humidity for three 42 d periods between August 2018 and April 2019 (Van de Walle *et al* 2021). From these measurements, the Humidex Index is computed, providing a good estimate for feel-like temperature (Masterton and Richardson 1979). High relative humidity decreases a person's evaporation ability and thereby the effectiveness of the body's natural cooling system (Malchaire *et al* 2000, Hass *et al* 2016). Particularly in hot and humid cities like Kampala, high values of the Humidex Index might cause dangerous health conditions. We therefore focus on extreme heat recorded at the different stations, and explain the observed patterns based on relevant satellite-derived earth observations. For example, vegetation is known to generally play a twofold role, decreasing temperature but enhancing humidity by transpiration (Hass *et al* 2016). Results are discussed from two different perspectives: insights in spatial heterogeneity of heat in Kampala and occurrences of heat above great discomfort thresholds among different urban environments.

2. Methods

2.1. iButton observations
The iButton sensor, a product of Maxim Integrated, is a low-cost sensor containing a temperature and humidity logging system (Hubbart *et al* 2005). With a logging frequency and data accuracy programmed at 15 min and 11 bit respectively, each sensor can store 42 consecutive days of data. Afterwards, a manual download is required. To protect the sensors from radiation and splash water, they are shielded by a folded thin light reflective film (figure S1 available online
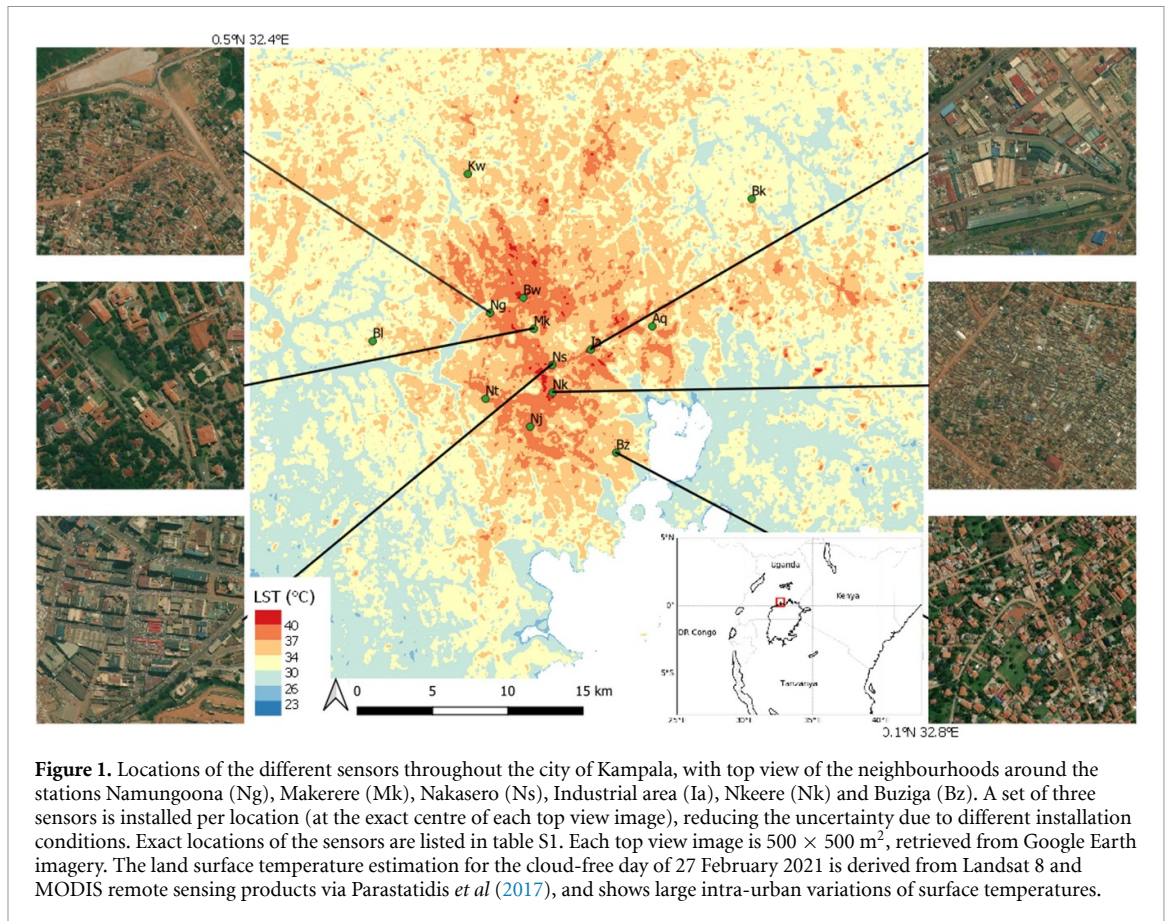
Figure 1. Locations of the different sensors throughout the city of Kampala, with top view of the neighbourhoods around the stations Namungoona (Ng), Makerere (Mk), Nakasero (Ns), Industrial area (Ia), Nkeere (Nk) and Buziga (Bz). A set of three sensors is installed per location (at the exact centre of each top view image), reducing the uncertainty due to different installation conditions. Exact locations of the sensors are listed in table S1. Each top view image is 500×500 m^2, retrieved from Google Earth imagery. The land surface temperature estimation for the cloud-free day of 27 February 2021 is derived from Landsat 8 and MODIS remote sensing products via Parastatidis *et al* (2017), and shows large intra-urban variations of surface temperatures.

at stacks.iop.org/ERL/17/024004/mmedia), designed and produced by the Maryland Institute College of Art and Johns Hopkins University. The sensor-containing shields are zip-tied preferably to a wooden material, at about 2 m height and at a shaded location (table S1). In this study we reused the material of the observational campaign by Scott *et al* (2017) held in Nairobi, Kenya.

The resulting network of 45 sensors installed throughout the city of Kampala (figure 1) aimed at properly representing the city's surface heterogeneity. Besides a good spatial coverage of both openly and densely built environments, the choice of sensors location also considered the security of the sensors from vandalism. Preferred locations thus included schools or houses of local acquaintances. At each location, a set of three sensors were installed close together, reducing the uncertainty of the triple-sensor-mean due to different installation conditions such as attachment material, shade fraction or ground cover. For each location, the 15 min resolution triple-sensor-mean information is reduced to the minimum and maximum values per day. In addition, the daily mean is computed as the average over 24 h. Three downloading rounds provided data for 3 periods of 42 d each between August 2018 and April 2019 (figure S2). For further analyses, daily minimum and daily maximum values are computed as the averages over all 3×42 d, still referred to as daily minimum and daily maximum

values. These periods do not cover a full year, yet we monitored humidity and temperature for both dry and wet seasons. The intra-seasonal variations in temperature and humidity are generally rather limited in the region (figure S3). On a longer timescale, warm spells can occur, with the start of 2019 as an example. The second of our observational periods covers that period (figure S3). Due to a slightly different downloading moment, measurement periods may slightly differ for locations located far from each other. In addition, some data is missing for the second and third periods due to technical issues, especially low battery. At the end of the third period, 32 out of 45 sensors remained active.

In addition, one sensor set was put indoor at the informal settlement of Acholi Quarters. The building is a concrete block, no windows, an iron door and iron roof sheets. Given the fact that it is only one site, results are qualitatively described in the discussion section.

2.2. Measurement quality

The manufacturer's evaluation of the iButtons reports a thermochron and hygrochron accuracy of 0.5 °C and 5% respectively. This is confirmed by calculating the mean deviation per sensor triple, explained and summarized in table S2. In addition, the triple-sensor-mean is evaluated against the Makerere automatic weather station data, part of the TAHMO

network (van de Giesen *et al* 2014). With an overall temperature bias of 0.10 °C, 0.11 °C and 0.53 °C in the three periods, and relative humidity bias of −2.50%, −2.66% and −1.43%, the iButton sensors tend to slightly overestimate the air temperature and underestimate humidity. This however varies throughout the day as observed nighttime temperatures by the iButton sensors are higher than the ones measured by the automatic weather station, while observed daytime temperatures are lower (figure S4). This results in an underestimation of the diurnal temperature range. Nighttime relative humidity is underestimated by ∼4%, but daytime observations compare well to the Makerere automatic weather station.

2.3. Humidex index

To better estimate the human-experienced heat, the Humidex Index (hereafter referred to as 'Humidex', H) is computed every 15 min from observations of both temperature (T in °C) and relative humidity (RH in %), following Masterton and Richardson (1979):

$$H(T, RH) = T + \frac{5}{9}\left(6.112 \, \frac{RH}{100} \, 10^{\frac{7.5 \, T}{237.7+T}} - 10\right). \tag{1}$$

The resulting quantity increases non-linearly with both air temperature and relative humidity, and can be understood as feel-like temperature in degrees Celsius. Humidex values above 40 °C lead to 'great discomfort', values exceeding 45 °C are 'dangerous' (Masterton and Richardson 1979). Humidex information is reduced to the minimum and maximum values per day, as well as the daily mean which is the average over 24 h.

2.4. Explanatory variables

We aim to explain spatial Humidex patterns by comparing them against potential explanatory factors, including distance to the lake, vegetation presence, built-up fraction, surface elevation, population density and surface albedo (figure S5). The choice of each of these six factors is argued below. First, located next to Lake Victoria, Kampala is affected by a daytime lake breeze developing on a daily basis (Thiery *et al* 2015, 2016, 2017, Brousse *et al* 2020, Van de Walle *et al* 2020, Woodhams *et al* 2021). The distance of the sensors to the lake is therefore used to account for different onsets of cooling. Second, hills can optimally benefit from cooling winds, lower regions cannot. In addition, these low areas are typically wetlands, providing opportunities for urban farming, but also humidifying the air (Kabumbuli and Kiwazi 2009). Therefore, a digital elevation model at 30 m horizontal resolution is retrieved from the Shuttle Radar Topography Mission (SRTM, Farr *et al* 2007) as a potential explanatory variable. Third, the presence of

vegetation can counteract the urban heat island effect, for example by evaporative cooling (Oke 1982). The normalized digital vegetation index (NDVI) ranging from 0 to 1, is used as a proxy for the fraction of surface covered by vegetation. This product is derived from the Moderate Resolution Imaging Spectroradiometer (MODIS) onboard the Terra satellite with a horizontal resolution of 250 m. This satellite overpasses Kampala at 10:30 AM and PM local time. Our analysis uses the median value of two years, 2018–2019, overlapping the observation period. No temporal variation is taken into account, assuming little seasonal variation in this tropical area and keeping the focus to the spatial heterogeneity. Fourth, due to the high heat storage capacity of building materials, densely built areas can largely influence local temperatures (Oke 1973). As a proxy for this building density, impervious surface area (ISA) fraction is retrieved from the Global Man-made Impervious Surface (GMIS) dataset (De Colstoun *et al* 2017). For the target year 2010, the GMIS product analysed all cloud-free images from Landsat 5 and 7, inheriting the high horizontal resolution of 30 m. A strong correlation is expected, yet the abundance of bare soil often challenges satellite instruments to properly represent ISA (Van de Walle *et al* 2021). Fifth, anthropogenic heat, mainly from domestic and transportation fuel use, is produced in highly populated areas (Taha 1997, Stewart and Kennedy 2015). The population density of the greater Kampala region, formally available per district for the year 2014 (Uganda Bureau of Statistics 2014, Hemerijckx *et al* 2020), is translated to a 30 m resolution grid. Sixth, the MODIS instrument also provides directional hemispherical (black-sky) near-infrared albedo at 0.7–5.0 μm wavelength at 500 m horizontal resolution, possibly distinguishing different roofing types within the city of Kampala (Brest 1987).

If these variables can explain the observed Humidex variations, a simple statistical model could extrapolate operational weather station data to the entire city, providing heat stress information about hardly accessible locations such as informal settlements. Assuming linear behaviour, a multiple linear regression technique is applied, expressing the Humidex (H) in terms of the explanatory variables x_i:

$$H = \beta_0 + \sum_{i=1}^{N} \beta_i x_i, \tag{2}$$

where the Ordinary Least Squares method estimates the best fitting coefficients $\hat{\beta}_i$ based on the observations. Initially, all N explanatory variables are included, but a t-test decides on the elimination of the least significant variable. This backward elimination continues iteratively until all explanatory variables are significant at 95% confidence level. Ultimately, the remaining multiple linear regression model no

longer suffers from multicollinearity, ensuring its coefficients to be optimally stable (Halinski and Feldt 1970).

2.5. Local climate zones

In addition to this quantitative approach, locations are classified based on the building structure, land cover and human activity according to the LCZ classification scheme (Stewart and Oke 2012, Brousse *et al* 2019, see table S1). The outskirts stations Buloba (Bl), Kawanda (Kw), Bukerere (Bk) and Buziga (Bz) are located in open low-rise environments (LCZ 6), defined by small (3–10 m) buildings with abundant plant cover (Stewart 2011). The campus of the Makerere University (Mk) is classified as open mid-rise class (LCZ 5), characterized by open arrangement of 3–9 story buildings and abundant plant cover. The Industrial Area (Ia) station is located in a large low-rise (LCZ 8) class, characterized by extensive paved surfaces between large, low buildings, often with an industrial or commercial function. The Nakasero (Ns) station is located in compact mid-rise (LCZ 2) class, defined by buildings of 10–25 m separated by narrow streets and inner courtyards, and with few or no trees. In addition, we classify the stations in Namungooma (Ng), Bwaise (Bw) and Najjanankumbi (Nj) as compact low-rise (LCZ 3) and Nateete (Nt), Nkeere (Nk) and Acholi Quarters (Aq) as lightweight low-rise (LCZ 7), often called informal settlements or slums. Both classes consist of small buildings tightly packed along narrow streets with no or little vegetation. Typical for the latter class are the lightweight building materials (thatch, wood or corrugated metal) and often formless arrangement of the buildings (Stewart 2011).

3. Results

Measurements show clear differences in Humidex values at the different sensor locations (figures 2(g)–(i)). For example, the average Humidex varies between 30.6 °C and 32.1 °C for the urban stations, except for the Makerere (Mk) station, located near the city centre, with a substantially lower average Humidex (29.0 °C). Also the city's outskirts, represented by Buloba (Bl), Bukerere (Bk) and Kawanda (Kw) stations, are cooler (29.3 °C–29.9 °C, figure 2(h)). At night (figure 2(g)), both the city outskirts and Makerere are cool, in contrast with high Humidex values observed nearby central stations. Particularly the industrial area (Ia), Nakasero (Ns), Namungoona (Ng) and Nkeere (Nk) experience warm nights, with differences up to 2.3 °C compared to Makerere. The intra-urban heterogeneity is most pronounced when comparing daily maximum Humidex values (figure 2(i)), ranging from 34.1 °C at Makerere to 41.6 °C at Najjanankumbi.

The observed Humidex heterogeneity is a result of intra-urban temperature and relative humidity variations. The latter are considered at times of daily minimum and maximum Humidex (figures 2(a), (d) and (c), (f) respectively). Around sunrise, when Humidex reaches its minimum, the air temperature almost entirely determines the Humidex variations between the sensor sites, with the urban air being clearly hotter and drier than at the outskirts (figures 2(a), (d) and (g)). Specific humidity between those sites is similar (not shown). Around noon, when Humidex reaches its maximum, the situation is different. Then, the highest air temperatures are observed at Nateete (Nt), Nkeere (Nk) and Acholi Quarters (Aq, figure 2(c)), all classified as lightweight low-rise LCZ 7. These locations also have the lowest relative humidity (figure 2(f)). While the temperature at Najjanankumbi (Nj, compact low-rise LCZ 3) is very similar to the temperatures at Nateete or Nkeere, it has a clearly higher Humidex (figure 2(i)). This can be explained by Najjanankumbi's high relative humidity compared to Natalee and Nkeere. We therefore need both temperature and relative humidity to properly explain spatial variations in heat. Importantly, neither Najjanankumbi's air temperature or relative humidity is exceptional compared to other stations such as Nkeere or Makerere: the temperature distribution is similar to the one at Nkeere (figure S6(c)), and relative humidity values exceeding 70% occur as frequent at Makerere (figure S6(f)). Instead, it is the combination of both compound drivers that creates high maximum Humidex values in Najjanankumbi (figure S6(i), Zscheischler *et al* 2018, 2020).

Relating the observed Humidex heterogeneity to the LCZ classification, the open low-rise (LCZ 6) environments, together with the open mid-rise Makerere University campus (LCZ 5), report generally lowest temperature, highest relative humidity and lowest Humidex values (figure 2). These cool environments contrast with the warm compact and lightweight low-rise classes (LCZ 3 and LCZ 7), as well as the compact mid-rise central business centre (LCZ 2). Kampala's industrial area (Ia, LCZ 8) is rather warm at night, but shows relatively mild temperatures during daytime. Especially poorly vegetated and compactly built neighbourhoods in Kampala are thus more prone to heat stress than the outskirts or Makerere station.

Intra-urban differences are especially relevant when considering extreme heat (figure 3). Concretely, Makerere (Mk) has no single day with the Humidex exceeding the 'great discomfort' threshold of 40 °C, it occurs in 2%–16% of the observed days in the outskirts stations Bukerere (Bk), Kawanda (Kw), Buloba (Bl) and Buziga (Bz), and 14%–67% in the stations located in densely built areas, in particular in Nkeere (Nk), Acholi Quarters (Aq) and Najjanankumbi (Nj) (in 50%–67% of the observed days). Looking at days
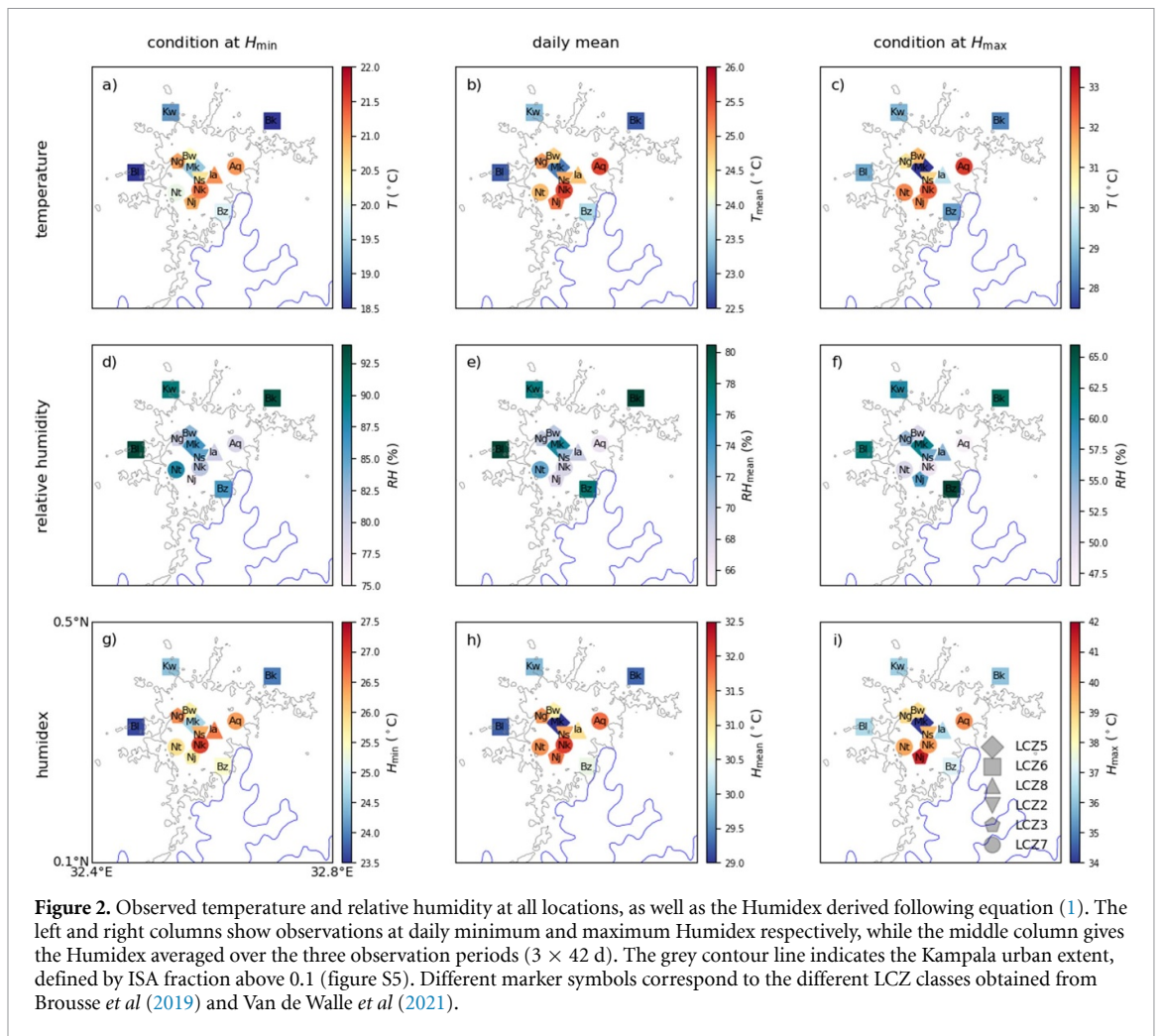
Figure 2. Observed temperature and relative humidity at all locations, as well as the Humidex derived following equation (1). The left and right columns show observations at daily minimum and maximum Humidex respectively, while the middle column gives the Humidex averaged over the three observation periods (3 × 42 d). The grey contour line indicates the Kampala urban extent, defined by ISA fraction above 0.1 (figure S5). Different marker symbols correspond to the different LCZ classes obtained from Brousse *et al* (2019) and Van de Walle *et al* (2021).

with maximum Humidex exceeding 45 °C, the 'dangerous' threshold, Bwaise (Bw), Najjanankumbi (Nj) and to a lesser extent Nkeere (Nk) stand out, with occurrences of 17%, 12% and 4% of the observed days, respectively.

Not only for daily maximum Humidex, also for daily minimum or average Humidex, Nkeere (Nk), Acholi Quarters (Aq) and Namungoona (Ng) show highest exceedance frequencies of all Humidex thresholds (figure S7). When also accounting for the duration of exceedance by considering the hours above a certain threshold (figure S8, top), or for the heat intensity by computing the mean heat-degree-hours (figure S8, bottom), the densely built environments often experience extreme heat (1%–10% of the observed time), especially in Najjanankumbi (Nj).

The intra-urban heterogeneous Humidex values correlates with six proposed explanatory variables (figure S9). Strongest correlations are found between Humidex and NDVI as well as ISA fraction. Moderate negative correlations of −0.5 to −0.65 are found between Humidex and near-infrared albedo, while Humidex and population density are positively correlated, with values between 0.5 and 0.76. Smaller

correlations are found between Humidex and the proximity to the lake or elevation. Importantly, the explanatory variables are not independent from each other, with high ISA fractions prohibiting abundant vegetation (correlation of −0.93) while also implying lower near-infrared albedo due to the strongly modified land cover (correlation of −0.82, figure S10). Also population density is not independent from ISA fraction, NDVI or near-infrared albedo, with correlations of 0.71, −0.78 and −0.72, respectively. The elevation shows a moderate correlation of 0.51 with NDVI, probably related to Kampala's vegetated hills.

Due to this collinearity between the explanatory variables, the stepwise backward elimination procedure only retains NDVI as explanatory variable in the linear regression model for minimum, mean and maximum Humidex (figure 4). With $R^2 = 0.79$, the NDVI has a high explanatory power for minimum (early morning) Humidex, meaning that 79% of the the intra-urban Humidex variability can be explained. This explanatory power is similar for average (75%), but lower for maximum (midday) Humidex (52%).
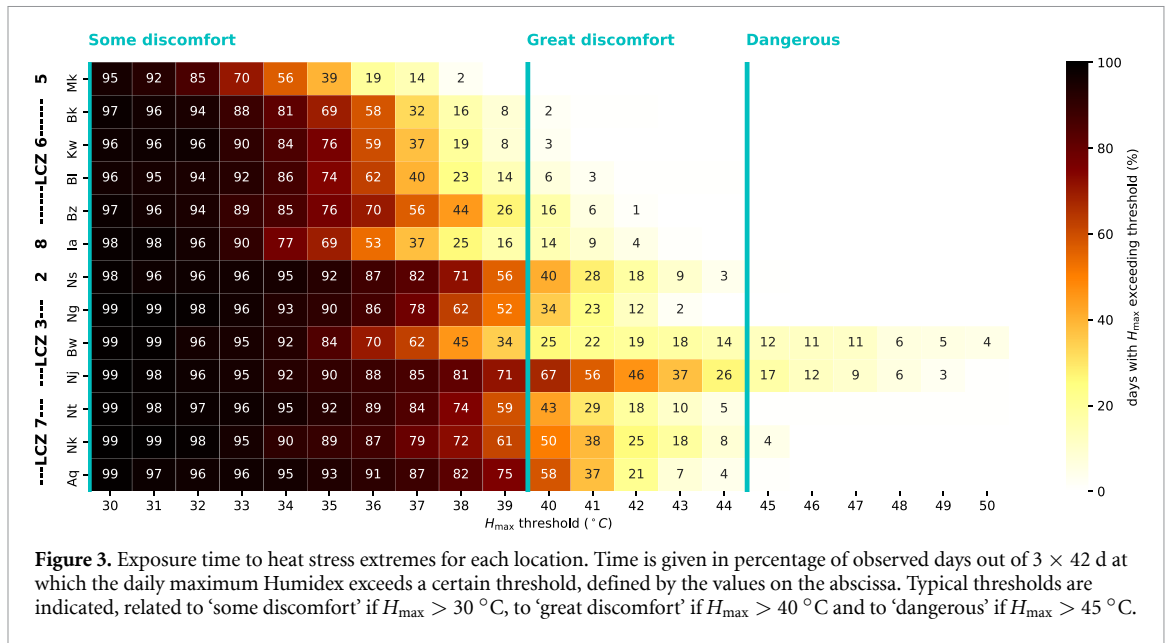
Some discomfort   **Great discomfort**   **Dangerous**

Loc.	30	31	32	33	34	35	36	37	38	39	40	41	42	43	44	45	46	47	48	49	50
Mk	95	92	85	70	56	39	19	14	2												
Bk	97	96	94	88	81	69	58	32	16	8		2									
Kw	96	96	96	90	84	76	59	37	19	8		3									
Bl	96	95	94	92	86	74	62	40	23	14	6	3									
Bz	97	96	94	89	85	76	70	56	44	26	16	6	1								
Ia	98	98	96	90	77	69	53	37	25	16	14	9	4								
Ns	98	96	96	96	95	92	87	82	71	56	40	28	18	9	3						
Ng	99	99	98	96	93	90	86	78	62	52	34	23	12	2							
Bw	99	99	96	95	92	84	70	62	45	34	25	22	19	18	14	12	11	11	6	5	4
Nj	99	98	96	95	92	90	88	85	81	71	67	56	46	37	26	17	12	9	6	3	
Nt	99	98	97	96	95	92	89	84	74	59	43	29	18	10	5						
Nk	99	99	98	95	90	89	87	79	72	61	50	38	25	18	8	4					
Aq	99	97	96	96	95	93	91	87	82	75	58	37	21	7	4						

H_{max} threshold (°C)

days with H_{max} exceeding threshold (%)

(LCZ annotations at left: 5, LCZ 6, 8, 2, LCZ 3, LCZ 7)

Figure 3. Exposure time to heat stress extremes for each location. Time is given in percentage of observed days out of 3×42 d at which the daily maximum Humidex exceeds a certain threshold, defined by the values on the abscissa. Typical thresholds are indicated, related to 'some discomfort' if $H_{max} > 30$ °C, to 'great discomfort' if $H_{max} > 40$ °C and to 'dangerous' if $H_{max} > 45$ °C.
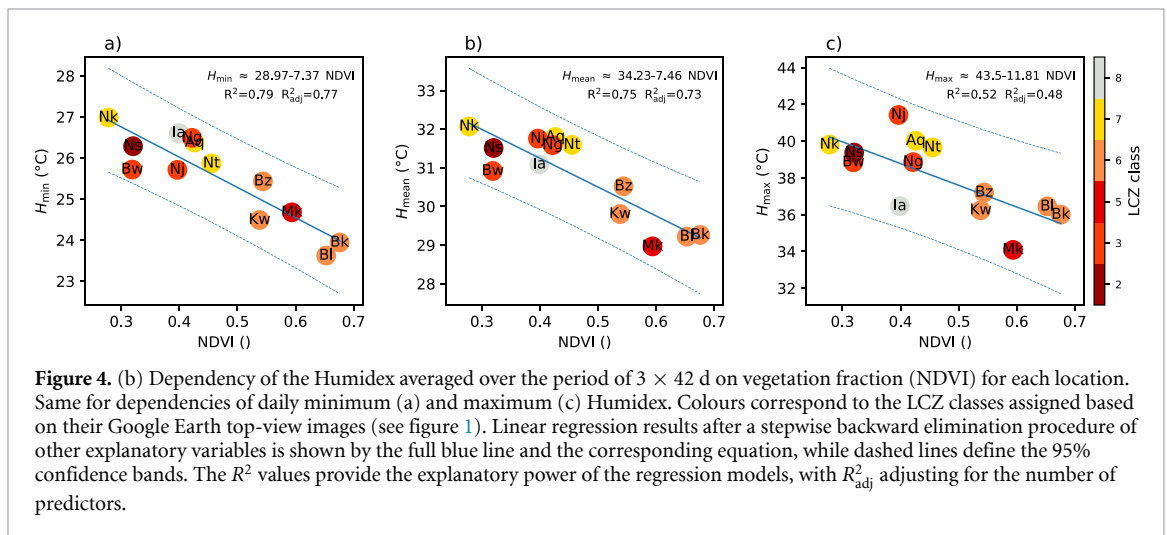
Figure 4. (b) Dependency of the Humidex averaged over the period of 3×42 d on vegetation fraction (NDVI) for each location. Same for dependencies of daily minimum (a) and maximum (c) Humidex. Colours correspond to the LCZ classes assigned based on their Google Earth top-view images (see figure 1). Linear regression results after a stepwise backward elimination procedure of other explanatory variables is shown by the full blue line and the corresponding equation, while dashed lines define the 95% confidence bands. The R^2 values provide the explanatory power of the regression models, with R^2_{adj} adjusting for the number of predictors.

a) $H_{min} \approx 28.97 - 7.37$ NDVI, $R^2 = 0.79$ $R^2_{adj} = 0.77$

b) $H_{mean} \approx 34.23 - 7.46$ NDVI, $R^2 = 0.75$ $R^2_{adj} = 0.73$

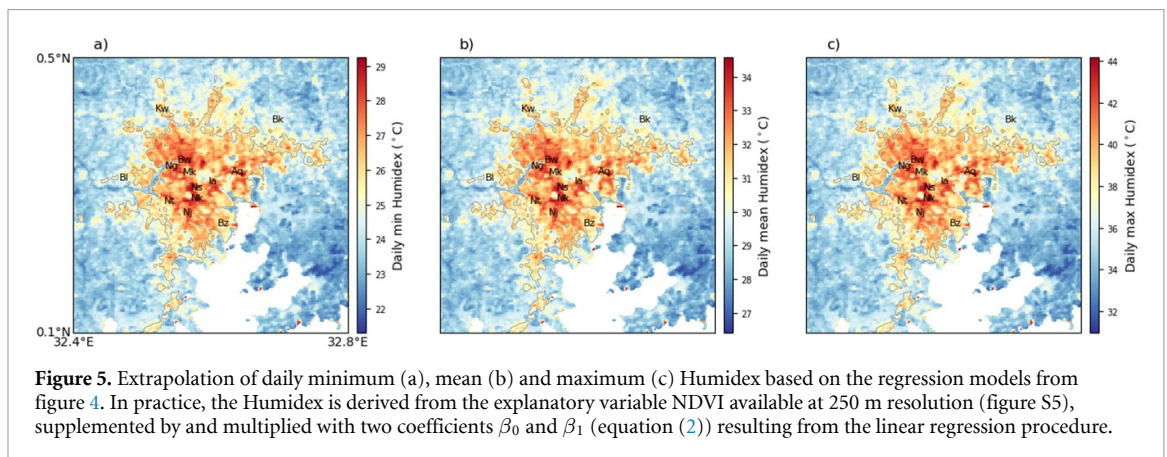c) $H_{max} \approx 43.5 - 11.81$ NDVI, $R^2 = 0.52$ $R^2_{adj} = 0.48$

Figure 5. Extrapolation of daily minimum (a), mean (b) and maximum (c) Humidex based on the regression models from figure 4. In practice, the Humidex is derived from the explanatory variable NDVI available at 250 m resolution (figure S5), supplemented by and multiplied with two coefficients β_0 and β_1 (equation (2)) resulting from the linear regression procedure.

The explanatory power of NDVI allows us to apply the regression model by extrapolating the point observations of minimum, mean and maximum Humidex to the greater Kampala region (figure 5). This map provides information on the spatial heterogeneity of heat stress in Kampala.

4. Discussion

With average intra-urban differences of 1.2 °C, and an afternoon difference of 6.4 °C on average, the Humidex Index is heterogeneously distributed over the city of Kampala. These large intra-urban differences

are also reflected in the number of days exposed to extreme heat. At some locations, daily maximum heat stress exceeds the great discomfort level, defined by Humidex >40 °C, for more than 50% of the 3 × 42 observation days. In comparison, for the same period, this level was never reached at the Makerere station and only a few times in the city outskirts. Moreover, we identified the regions in Kampala that are most prone to heat, pointed to non-vegetated, densely built environments using linear regression and extrapolated the result to the greater Kampala region. The resulting map could complement remote sensing products for land surface temperature, adding information about 2 m temperature and relative humidity combined in the Humidex Index. Such map can guide anticipatory action plans that help reduce the impact of heatwaves, by providing concrete information about heat-prone areas. With special attention to those heat-prone areas, a heat action plan commits to public awareness about heat risks (Singh *et al* 2019), which has been demonstrated to be successful in reducing heat-related mortality in Ahmedabad, India (Knowlton *et al* 2014, Hess *et al* 2018, Nastar 2020). In addition, a heat action plan also accounts for the vulnerability of urban dwellers. In general, densely built and informal settlements house a large part of the population belonging to the lower socioeconomic status with income and livelihood insecurity, making them particularly vulnerable (Vermeiren *et al* 2012, Lwasa *et al* 2018, Hemerijckx *et al* 2020, Twinomuhangi *et al* 2021). An important factor increasing their vulnerability is the housing infrastructure, not offering any protection to heat. As a test case, we collected heat observations inside a building in the informal settlement of Acholi Quarters during the three periods of the observational campaign. Instead of offering protection against heat, the house seems to act like a heat trap for evening and nighttime heat, times when people are living inside. Only heat before and at noon is slightly lower then outside observations (figure S11). A recent study in Ghana investigated indoor temperatures and concluded large effects of building materials (Wilby *et al* 2021).

A second implication concerns urban adaptation planning, and follows from our finding that Kampala's intra-urban varying heat is strongly correlated with NDVI, explaining up to 77% of the intra-urban variability in daily mean Humidex. Despite their elimination in the regression analysis due to clear correlations with NDVI, other explanatory variables, particularly ISA fraction, might also be important. From a Local Climate Zone perspective (Stewart and Oke 2012), the warmest stations were found in compact LCZ classes, characterized by densely built environments with little or no vegetation. In particular, they include compact mid-rise (LCZ 2), compact low-rise (LCZ 3) and lightweight (LCZ 7) classes. Cooler environments in Kampala include

open low-rise (LCZ 6) and open mid-rise (LCZ 5) classes. Overall, sparsely built and highly vegetated areas thus experience substantially lower heat, with an observed mean difference of 6.4 °C in the afternoon. This result implies that greening the city could mitigate urban heat (Bowler *et al* 2010, Demuzere *et al* 2014, Gunawardena *et al* 2017). Yet, a more detailed investigation is needed to the overall effects of different types of vegetation on human well-being, including the effects on local climate, air quality and aesthetics (Salmond *et al* 2016). In fact, the Kampala City Council Authority (KCCA) announced plans to plant 0.5 million trees in Kampala as part of its climate action strategy, which is developed with stakeholders. Concretely, the strategy has embarked on taking stock of the trees in the city coupled with mapping of natural assets in the city to form the basis for implementation of the climate strategy. This climate action strategy is challenging, especially because most available land is in Kampala's residential areas where urban tree canopies are already evident, while we showed that the need for cooling is most urgent in densely built environments and informal settlements. Yet, Lwasa *et al* (2014) claimed the potential for expansion of tree canopy cover in the city's densely built and most vulnerable areas as well. For this, initiatives from local actors and inhabitants should be strongly supported, which can only be achieved by properly informing the inhabitants (Hintz *et al* 2018), followed by incentive-based mechanisms that allow the planting, nurturing and taking care of the trees in dense settlements by the developers. As an example, some local politicians and influencers challenged Ugandans via (social) media to commemorate every marriage, death, birth and graduation by planting a personal tree.

Five important challenges have to be addressed by future research. First, besides Humidex, many other indices can describe heat as a combination of multiple factors influencing heat stress. To explain human discomfort, many factors play a role, including air temperature and humidity (Epstein and Moran 2006, Barnett *et al* 2010, Fischer *et al* 2012, Lange *et al* 2020), but also wind, radiation, physiological factors, physical activity and clothing (Quayle and Doehring 1981, Roth 2007, Potchter *et al* 2018). This study includes temperature and relative humidity only, with differences between similar heat measures shown to be small (Barnett *et al* 2010). Second, to explain the observed Humidex values, vegetation is an important factor with a twofold role. On the one hand, enhanced transpiration by vegetation implies air temperature cooling, tending to reduce the Humidex. On the other hand, enhanced transpiration increases the humidity which contributes to a higher Humidex (Hass *et al* 2016). By showing a strong negative correlation between Humidex and vegetation fraction (NDVI), we conclude that the first role dominates. Concretely, adding vegetation might increase

the relative humidity, the reduction in temperature is superior. Yet this study did not quantitatively investigate the interplay between temperature and humidity in detail. A study in Indiana, US, highlighted the importance of different vegetation types and structures to unravel this interplay (Souch and Souch 1993). Individual tree species or open grass areas have the largest cooling effect, street trees the smallest. Also in Kampala, different vegetation types could be obtained or derived from detailed landcover maps. Even if such land-cover maps would help the interpretation of the results by further linking heat to different vegetation types, our study already integrates the level of greenness and vegetation by using NDVI and ISA variables. Third, our observational iButton network was only active for a short 3 × 42 d period, during a warm spell. Results might therefore slightly overestimate the multi-year situation. In addition, our network was not complete to cover all neighbourhoods. Moreover, paper-made shields might not be sufficient to perfectly protect the sensor from direct sunlight. However, the role of irradiation of the sensor shields is not investigated since the time of the day at which the sensor is sunlit/shaded was not inventorized. Deviations between the sensor triple observations are small, suggesting that the effect of irradiation is also small. Despite the good performance of our sensors, we still recommend using a pair or triplet of iButtons per site, regardless of the reduced number of observational sites. Besides our iButton network, weather station observations are increasingly conducted in the region via the TAHMO project (van de Giesen *et al* 2014), yet the meteorological network is still sparse. Besides TAHMO, the availability of crowd-sourced weather data has grown worldwide in recent years, offering possibilities for high-resolution observational urban heat studies (Muller *et al* 2015, Chapman *et al* 2017, Meier *et al* 2017, Venter *et al* 2020, Fenner *et al* 2021). Unfortunately, no studies have collected and analysed such data in tropical Africa. Fourth, there is no common definition of heatwaves (Hintz *et al* 2018). This study investigated different definitions including total days/nights or hours with extreme heat and heat degree hours. Similar to Europe, the US and Australia, a region-specific heatwave definition should be derived from mortality and morbidity studies (Kovats and Hajat 2008, Guo *et al* 2014, Mora *et al* 2017, Xu and Tong 2017, Li *et al* 2020). Yet such studies are currently completely lacking for Africa (Harrington and Otto 2020). In addition, given an appropriate metric, health impact research should also question whether certain thresholds are meaningful for different regions of interest based on more metabolic information on people living in these regions. In this study we provided the general (dis)comfort levels accompanying the Humidex Index. Yet, experienced heat is expected to depend on the region of the world (Potchter *et al* 2018).

In some areas, heat is experienced as 'great discomfort' below/above the proposed 40 °C threshold. Surveys in Dar es Salaam (Tanzania) suggested that the comfort range was well above the one defined in temperate climates (Ndetto and Matzarakis 2017). While concrete information about applicable levels/thresholds for Kampala is lacking, this study provisionally explored different thresholds for the Humidex Index, ranging from 30 °C to 50 °C. Fifth, though the explanatory power of the regression model is high (75%), four factors could lead to improvements of the model. First, it would definitely benefit from more observations, perhaps supplemented by remote sensing data. Second, this study explored only six explanatory variables, but more could be added, for example providing information about building morphology or materials. Though this information is implicitly already included in LCZ classes, high resolution material maps will possibly appear in the near future. Third, future research should investigate the robustness of the model when adding new observations. Fourth, we found strong collinearity between different explanatory factors, challenging the causality between vegetation fraction and Humidex Index in our linear regression model.

5. Conclusion

From a network of low-cost temperature and humidity sensors, we compute the Humidex Index, quantifying the heat stress throughout the city. Daily minimum, mean, maximum as well as extreme heat stress are heterogeneously distributed over the city, with poorly vegetated and densely built-up environments being the most heat-prone areas. Their inhabitants, generally vulnerable people due to their socioeconomic status, are often exposed to great discomfort or even dangerous heat. Future research should bridge the gap to indoor heat and its dependence on house structure and building materials. Two recommendations follow from this study: to mitigate heat stress, urban greening should be considered in urban planning strategies, and urban heat action plans should account for the large intra-urban heat stress variations.

Data availability statement

The data that support the findings of this study are openly available at the following URL/DOI: http://doi.org/10.5281/zenodo.5105570.

Other products are publicly available online: the TAHMO automatic weather station data at Makerere University (https://tahmo.org/climate-data/), SRTM Digital elevation model (https://gee.stac.cloud/6FKBuAFUoXyYMZCUkttkJ5VuS8cQd?t = bands), MODIS MYD13Q1 product for NDVI (https://modis.gsfc.nasa.gov/data/dataprod/mod13.php), GMIS

built-up fraction (https://sedac.ciesin.columbia.edu/data/set/ulandsat-gmis-v1), Kampala population density (https://unstats.un.org/unsd/demographic/sources/census/wphc/Uganda/UGA-2016-05-23.pdf) and MODIS MCD43A3 v6 albedo product (https://modis.gsfc.nasa.gov/data/dataprod/mod43.php). In addition, the land surface temperature is derived from Landsat 8 and MODIS, and can be retrieved online via: http://rslab.gr/downloads_LandsatLST.html

Acknowledgments

Code availability

Scripts to process the raw temperature and relative humidity observation are provided via https://github.com/jonasvdw/kampalasensors.

ORCID iDs

J Van de Walle ● https://orcid.org/0000-0002-7819-7419
O Brousse ● https://orcid.org/0000-0002-7364-710X
C Brimicombe ● https://orcid.org/0000-0001-5550-1556
M Demuzere ● https://orcid.org/0000-0003-3237-4077
S Lwasa ● https://orcid.org/0000-0003-4312-2836
H Misiani ● https://orcid.org/0000-0002-5414-3125
G Nsangi ● https://orcid.org/0000-0002-9324-106X
W Thiery ● https://orcid.org/0000-0002-5183-6145
B F Zaitchik ● https://orcid.org/0000-0002-0698-0658
N P M van Lipzig ● https://orcid.org/0000-0003-2899-4046

References

Amou M, Gyilbag A, Demelash T and Xu Y 2021 Heatwaves in Kenya 1987–2016: facts from chirts high resolution satellite remotely sensed and station blended temperature dataset *Atmosphere* **12** 37

Asefi-Najafabady S, Vandecar K L, Seimon A, Lawrence P and Lawrence D 2018 Climate change, population and poverty: vulnerability and exposure to heat stress in countries bordering the great lakes of Africa *Clim. Change* **148** 561–73

Barnett A G, Tong S and Clements A C 2010 What measure of temperature is the best predictor of mortality? *Environ. Res.* **110** 604–11

Bowler D E, Buyung-Ali L, Knight T M and Pullin A S 2010 Urban greening to cool towns and cities: a systematic review of the empirical evidence *Landscape Urban Plan.* **97** 147–55

Brest C L 1987 Seasonal albedo of an urban/rural landscape from satellite observations *J. Appl. Meteorol. Climatol.* **26** 1169–87

Brousse O *et al* 2019 Using local climate zones in Sub-Saharan Africa to tackle urban health issues *Urban Clim.* **27** 227–42

Brousse O, Wouters H, Demuzere M, Thiery W, Van de Walle J and van Lipzig N P 2020 The local climate impact of an African city during clear-sky conditions—implications of the recent urbanization in Kampala (Uganda) *Int. J. Climatol.* **40** 4586–608

Campbell S, Remenyi T A, White C J and Johnston F H 2018 Heatwave and health impact research: a global review *Health Place* **53** 210–8

Ceccherini G, Russo S, Ameztoy I, Francesco Marchese A and Carmona-Moreno C 2017 Heat waves in Africa 1981–2015, observations and reanalysis *Nat. Hazards Earth Syst. Sci.* **17** 115–25

Chapman L, Bell C and Bell S 2017 Can the crowdsourcing data paradigm take atmospheric science to a new level? A case study of the urban heat island of London quantified using Netatmo weather stations *Int. J. Climatol.* **37** 3597–605

De Colstoun E C B, Huang C, Wang P, Tilton J C, Phillips J, Niemczura S, Ling P-Y and Wolfe R 2017 *Documentation for the Global Man-made Impervious Surface (GMIS) Dataset From Landsat* (Palisades, NY: NASA Socioeconomic Data and Applications Center (SEDAC))

Demuzere M *et al* 2014 Mitigating and adapting to climate change: multi-functional and multi-scale assessment of green urban infrastructure *J. Environ. Manage.* **146** 107–15

Dosio A, Mentaschi L, Fischer E M and Wyser K 2018 Extreme heat waves under 1.5 °C and 2 °C global warming *Environ. Res. Lett.* **13** 054006

Epstein Y and Moran D S 2006 Thermal comfort and the heat stress indices *Ind. Health* **44** 388–98

Farr T G *et al* 2007 The shuttle radar topography mission *Rev. Geophys.* **45** RG2004

Fenner D, Bechtel B, Demuzere M, Kittner J and Meier F 2021 CrowdQC+—a quality-control for crowdsourced air-temperature observations enabling world-wide urban climate applications *Front. Environ. Sci.* **9** 553

Fischer E M, Oleson K W and Lawrence D M 2012 Contrasting urban and rural heat stress responses to climate change *Geophys. Res. Lett.* **39** L03705

Green H, Bailey J, Schwarz L, Vanos J, Ebi K and Benmarhnia T 2019 Impact of heat on mortality and morbidity in low and middle income countries: a review of the epidemiological evidence and considerations for future research *Environ. Res.* **171** 80–91

Gunawardena K, Wells M and Kershaw T 2017 Utilising green and bluespace to mitigate urban heat island intensity *Sci. Total Environ.* **584–5** 1040–55

Guo Y *et al* 2014 Global variation in the effects of ambient temperature on mortality: a systematic evaluation *Epidemiology* **25** 781–9

Halinski R S and Feldt L S 1970 The selection of variables in multiple regression analysis *J. Educ. Meas.* **7** 151–7

Harrington L J, Frame D J, Fischer E M, Hawkins E, Joshi M and Jones C D 2016 Poorest countries experience earlier anthropogenic emergence of daily temperature extremes *Environ. Res. Lett.* **11** 055007

Harrington L J and Otto F E L 2020 Reconciling theory with the reality of African heatwaves *Nat. Clim. Change* **10** 796–8

Hass A L, Ellis K N, Reyes Mason L, Hathaway J M and Howe D A 2016 Heat and humidity in the city: neighborhood heat

index variability in a mid-sized city in the Southeastern United States *Int. J. Environ. Res. Public Health* **13** 117

Hemerijckx L-M, Van Emelen S, Rymenants J, Davis J, Verburg P H, Lwasa S and Van Rompaey A 2020 Upscaling household survey data using remote sensing to map socioeconomic groups in Kampala, Uganda *Remote Sens.* **12** 3468

Hess J J *et al* 2018 Building resilience to climate change: pilot evaluation of the impact of India's first heat action plan on all-cause mortality *J. Environ. Public Health* **2018** 7973519

Hintz M J, Luederitz C, Lang D J and von Wehrden H 2018 Facing the heat: a systematic literature review exploring the transferability of solutions to cope with urban heat waves *Urban Clim.* **24** 714–27

Huang C, Barnett A G, Wang X, Vaneckova P, Fitzgerald G and Tong S 2011 Projecting future heat-related mortality under climate change scenarios: a systematic review *Environ. Health Perspect.* **119** 1681–90

Hubbart J, Link T, Campbell C and Cobos D 2005 Evaluation of a low-cost temperature measurement system for environmental applications *Hydrol. Process.* **19** 1517–23

Im E-S, Pal J S and Eltahir E A 2017 Deadly heat waves projected in the densely populated agricultural regions of South Asia *Sci. Adv.* **3** e1603322

IPCC 2014 *Climate Change 2014 Part A: Global and Sectoral Aspects* (Cambridge: Cambridge University Press) p 1132

Jonsson P, Bennet C, Eliasson I and Selin Lindgren E 2004 Suspended particulate matter and its relations to the urban climate in Dar es Salaam, Tanzania *Atmos. Environ.* **38** 4175–81

Kabano P, Lindley S and Harris A 2021 Evidence of urban heat island impacts on the vegetation growing season length in a tropical city *Landscape Urban Plan.* **206** 103989

Kabumbuli R and Kiwazi F W 2009 Participatory planning, management and alternative livelihoods for poor wetland-dependent communities in Kampala, Uganda *Afr. J. Ecol.* **47** 154–60

Kampala Capital City Authority and Uganda Bureau of Statistics 2019 Statistical abstract for Kampala City: report prepared with support from Uganda Bureau of Statistics *Technical Report* pp 1–163 (available at: www.kcca.go.ug/media/docs/Statistical-Abstract-2019.pdf)

Knowlton K *et al* 2014 Development and implementation of South Asia's first heat-health action plan in Ahmedabad (Gujarat, India) *Int. J. Environ. Res. Public Health* **11** 3473–92

Kovats R S and Hajat S 2008 Heat stress and public health: a critical review *Annu. Rev. Public Health* **29** 41–55

Lange S *et al* 2020 Projecting exposure to extreme climate impact events across six event categories and three spatial scales *Earth's Future* **8** e2020EF001616

Li X, Stringer L C and Dallimer M 2021 The spatial and temporal characteristics of urban heat island intensity: implications for East Africa's urban development *Climate* **9** 51

Li Y, Schubert S, Kropp J P and Rybski D 2020 On the influence of density and morphology on the Urban Heat Island intensity *Nat. Commun.* **11** 1–9

Liu Z, Anderson B, Yan K, Dong W, Liao H and Shi P 2017 Global and regional changes in exposure to extreme heat and the relative contributions of climate and population change *Sci. Rep.* **7** 1–9

Lwasa S, Buyana K, Kasaija P and Mutyaba J 2018 Scenarios for adaptation and mitigation in urban Africa under 1.5 °C global warming *Curr. Opin. Environ. Sustain.* **30** 52–58

Lwasa S, Mugagga F, Wahab B, Simon D, Connors J and Griffith C 2014 Urban and peri-urban agriculture and forestry: transcending poverty alleviation to climate change mitigation and adaptation *Urban Clim.* **7** 92–106

Malchaire J, Kampmann B, Havenith G, Mehnert P and Gebhardt H 2000 Criteria for estimating acceptable exposure times in hot working environments: a review *Int. Arch. Occup. Environ. Health* **73** 215–20

Marcotullio P J, Keßler C and Fekete B M 2021 The future urban heat-wave challenge in Africa: exploratory analysis *Glob. Environ. Change* **66** 102190

Masterton J M and Richardson F 1979 *Humidex: A Method of Quantifying Human Discomfort due to Excessive Heat and Humidity* (Environment Canada, Atmospheric Environment) p 45

McGranahan G and Satterthwaite D 2014 *Urbanisation Concepts and Trends* vol 220 (JSTOR) (available at: www.jstor.org/stable/pdf/resrep01297.pdf?acceptTC=true&coverpage=false&addFooter=false)

Medina-Ramón M and Schwartz J 2007 Temperature, temperature extremes and mortality: a study of acclimatisation and effect modification in 50 US cities *Occup. Environ. Med.* **64** 827–33

Meier F, Fenner D, Grassmann T, Otto M and Scherer D 2017 Crowdsourcing air temperature from citizen weather stations for urban climate research *Urban Clim.* **19** 170–91

Mora C *et al* 2017 Global risk of deadly heat *Nat. Clim. Change* **7** 501–6

Muller C, Chapman L, Johnston S, Kidd C, Illingworth S, Foody G, Overeem A and Leigh R 2015 Crowdsourcing for climate and atmospheric sciences: current status and future potential *Int. J. Climatol.* **35** 3185–203

Nagendra H, Bai X, Brondizio E S and Lwasa S 2018 The urban south and the predicament of global sustainability *Nat. Sustain.* **1** 341–9

Nakamura K 1966 City temperature of Nairobi *J. Geogr.* **75** 316–25

Nastar M 2020 Message sent, now what? A critical analysis of the heat action plan in Ahmedabad, India *Urban Sci.* **4** 53

Ndetto E L and Matzarakis A 2017 Assessment of human thermal perception in the hot-humid climate of Dar es Salaam, Tanzania *Int. J. Biometeorol.* **61** 69–85

Oke T R 1982 The energetic basis of the urban heat island *Q. J. R. Meteorol. Soc.* **108** 1–24

Oke T 1973 City size and the urban heat island *Atmos. Environ.* **7** 769–79

Otto F E *et al* 2020 Challenges to understanding extreme weather changes in lower income countries *Bull. Am. Meteorol. Soc.* **101** E1851–60

Oudin Åström D, Bertil F and Joacim R 2011 Heat wave impact on morbidity and mortality in the elderly population: a review of recent studies *Maturitas* **69** 99–105

Parastatidis D, Mitraka Z, Chrysoulakis N and Abrams M 2017 Online global land surface temperature estimation from Landsat *Remote Sens.* **9** 1208

Potchter O, Cohen P, Lin T-P and Matzarakis A 2018 Outdoor human thermal perception in various climates: a comprehensive review of approaches, methods and quantification *Sci. Total Environ.* **631** 390–406

Quayle R and Doehring F 1981 Heat stress *Weatherwise* **34** 120–4

Richmond A, Myers I and Namuli H 2018 Urban informality and vulnerability: a case study in Kampala, Uganda *Urban Sci.* **2** 22

Roth M 2007 Review of urban climate research in (sub) tropical regions *Int. J. Climatol.* **27** 1859–73

Russo S, Marchese A F, Sillmann J and Immé G 2016 When will unusual heat waves become normal in a warming Africa? *Environ. Res. Lett.* **11** 054016

Saeed F, Schleussner C-F and Ashfaq M 2021 Deadly heat stress to become commonplace across South Asia already at 1.5 °C of global warming *Geophys. Res. Lett.* **48** e2020GL091191

Salmond J A *et al* 2016 Health and climate related ecosystem services provided by street trees in the urban environment *Environ. Health* **15** 95–111

Scott A A *et al* 2017 Temperature and heat in informal settlements in Nairobi *PLoS One* **12** 1–17

Singh R, Arrighi J, Jjemba E, Strachan K, Spires M and Kadihasanoglu A 2019 Heatwave guide for cities *Technical Report* (Geneva: Red Cross Red Crescent Climate Centre) (available at: www.climatecentre.org/downloads/files/IFRC Geneva/RCCC%20Heatwave%20Guide%202019%20A4%20RR%20ONLINE%20copy.pdf)

Souch C and Souch C 1993 The effect of trees on summertime below canopy urban climates: a case study Bloomington, Indiana *J. Arboric.* **19** 303–12

Stewart I D 2011 Redefining the urban heat island *PhD Thesis* University of British Columbia p 352 (available at: https://circle.ubc.ca/handle/2429/38069)

Stewart I D and Oke T R 2012 Local climate zones for urban temperature studies *Bull. Am. Meteorol. Soc.* **93** 1879–900

Stewart I and Kennedy C 2015 Estimating anthropogenic heat release from megacities *ICUC9–9th Int. Conf. on Urban Climate Held Jointly with the 12th Symp. on the Urban Environment* pp 20–24 (available at: www.meteo.fr/icuc9/LongAbstracts/gd5-1-2961311_a.pdf)

Taha H 1997 Urban climates and heat islands: albedo, evapotranspiration and anthropogenic heat *Energy Build.* **25** 99–103

Thiery W, Davin E L, Panitz H-J, Demuzere M, Lhermitte S and van Lipzig N 2015 The impact of the African Great Lakes on the regional climate *J. Clim.* **28** 4061–85

Thiery W, Davin E L, Seneviratne S I, Bedka K, Lhermitte S and Van Lipzig N P 2016 Hazardous thunderstorm intensification over Lake Victoria *Nat. Commun.* **7** 1–7

Thiery W, Gudmundsson L, Bedka K, Semazzi F H M, Lhermitte S, Willems P, van Lipzig N P M and Seneviratne S I 2017 Early warnings of hazardous thunderstorms over Lake Victoria *Environ. Res. Lett.* **12** 074012

Twinomuhangi R, Sseviiri H, Mulinde C, Mukwaya P I, Nimusiima A and Kato A M 2021 Perceptions and vulnerability to climate change among the urban poor in Kampala City, Uganda *Reg. Environ. Change* **21** 1–13

Uganda Bureau of Statistics 2014 *Uganda National Population and Housing Census* (Kampala: Uganda Bureau of Statistics (UBOS)) (available at: https://unstats.un.org/unsd/demographic/sources/census/wphc/Uganda/UGA-2016-05-23.pdf)

United Nations 2018 *World Urbanization Prospects 2018: Highlights* (ST/ESA/SER.A/421) (available at: https://population.un.org/wup/Publications/Files/WUP2018-Highlights.pdf)

United Nations 2019 *World Population Prospects 2019: Highlights* (Department of Economic and Social Affairs, Population Division) (available at: https://population.un.org/wpp/Publications/Files/WPP2019_Highlights.pdf)

van de Giesen N, Hut R and Selker J 2014 The Trans-African Hydro-Meteorological Observatory (TAHMO) *WIREs Water* **1** 341–8

Van de Walle J 2021 Can local fieldwork help to represent intra-urban variability of canopy parameters relevant for tropical African climate studies? *Theor. Appl. Climatol.* **146** 457–74

Van de Walle J, Thiery W, Brousse O, Souverijns N, Demuzere M and van Lipzig N P 2020 A convection-permitting model for the Lake Victoria Basin: evaluation and insight into the mesoscale versus synoptic atmospheric dynamics *Clim. Dyn.* **54** 1779–99

Van Leeuwen J M, Sekeramayi T, Martell C, Feinberg M and Bowersox-Daly S 2017 A baseline analysis of the Katanga slums: informing urban public policy in Kampala, Uganda *Afr. Popul. Stud.* **31** 2

Venter Z S, Brousse O, Esau I and Meier F 2020 Hyperlocal mapping of urban air temperature using remote sensing and crowdsourced weather data *Remote Sens. Environ.* **242** 111791

Vermeiren K, Van Rompaey A, Loopmans M, Serwajja E and Mukwaya P 2012 Urban growth of Kampala, Uganda: pattern analysis and scenario development *Landscape Urban Plan.* **106** 199–206

Vermeiren K, Vanmaercke M, Beckers J and Van Rompaey A 2016 ASSURE: a model for the simulation of urban expansion and intra-urban social segregation *Int. J. Geogr. Inf. Sci.* **30** 2377–400

Wilby R L *et al* 2021 Monitoring and moderating extreme indoor temperatures in low-income urban communities monitoring and moderating extreme indoor temperatures in low-income urban communities *Environ. Res. Lett* **16** 024033

WMO 1986 Guidelines on the selection of reference climatological stations from the existing cilmatological station network (available at: https://library.wmo.int/doc_num.php?explnum_id=9310)

Woodhams B J, Barrett P A, Marsham J H, Birch C E, Bain C, Fletcher J, Hartley A J and Webster S 2021 First aircraft observations of the lake Victoria lake–land breeze circulation from the HyVic pilot flight campaign *34th Conf. on Hurricanes and Tropical Meteorology* (AMS) (available at: https://ams.confex.com/ams/34HURR/meetingapp.cgi/Paper/386612)

Xu Z and Tong S 2017 Decompose the association between heatwave and mortality: which type of heatwave is more detrimental? *Environ. Res.* **156** 770–4

Zscheischler J *et al* 2018 Future climate risk from compound events *Nat. Clim. Change* **8** 469–77

Zscheischler J *et al* 2020 A typology of compound weather and climate events *Nat. Rev. Earth Environ.* **1** 333–47